Efficient formation of stratospheric aerosol for climate engineering by emission of condensible vapor from aircraft

Jeffrey R. Pierce,[1] Debra K. Weisenstein,[2] Patricia Heckendorn,[3] Thomas Peter,[3] and David W. Keith[4]

Received 13 May 2010; revised 11 July 2010; accepted 28 July 2010; published 22 September 2010.

[1] Recent analysis suggests that the effectiveness of stratospheric aerosol climate engineering through emission of non-condensable vapors such as SO_2 is limited because the slow conversion to H_2SO_4 tends to produce aerosol particles that are too large; SO_2 injection may be so inefficient that it is difficult to counteract the radiative forcing due to a CO_2 doubling. Here we describe an alternate method in which aerosol is formed rapidly in the plume following injection of H_2SO_4, a condensable vapor, from an aircraft. This method gives better control of particle size and can produce larger radiative forcing with lower sulfur loadings than SO_2 injection. Relative to SO_2 injection, it may reduce some of the adverse effects of geoengineering such as radiative heating of the lower stratosphere. This method does not, however, alter the fact that such a geoengineered radiative forcing can, at best, only partially compensate for the climate changes produced by CO_2. **Citation:** Pierce, J. R., D. K. Weisenstein, P. Heckendorn, T. Peter, and D. W. Keith (2010), Efficient formation of stratospheric aerosol for climate engineering by emission of condensible vapor from aircraft, *Geophys. Res. Lett.*, *37*, L18805, doi:10.1029/2010GL043975.

1. Introduction

[2] It may be possible to engineer an increase in the Earth's albedo by increasing the stratospheric aerosol burden. While such "geoengineering" entails novel environmental and security risks and cannot fully compensate for CO_2-driven warming (e.g. ocean acidification and hydrological cycle changes), it may nevertheless provide an important tool for managing climate risk [*Shepherd et al.*, 2009; *Blackstock et al.*, 2009; *Keith et al.*, 2010]. This has inspired recent research to quantify the unintended consequences of geoengineering [*Govindasamy and Caldeira*, 2000; *Govindasamy et al.*, 2002, 2003; *Matthews and Caldeira*, 2007; *Rasch et al.*, 2008a, 2008b; *Caldeira and Wood*, 2008; *Robock et al.*, 2008; *Tilmes et al.*, 2008, 2009; *Trenberth and Dai*, 2007; *Heckendorn et al.*, 2009]. If the costs and benefits of a geoengineering scheme are to be seriously considered, the scheme must be able to compensate for large radiative forcings such as a doubling of CO_2.

[3] The radiative forcing caused by the addition of aerosol to the stratosphere depends very strongly on aerosol size for at least two reasons (Figure 1). First, particle settling speed increases rapidly with radius, and faster settling causes shorter stratospheric lifetimes and therefore a smaller time-integrated radiative forcing per mass of aerosol delivered. Second, the amount of solar radiation scattered back to space depends strongly on the size of the scattering aerosol. Scattering intensity per unit aerosol mass decreases rapidly beyond an optimal radius of ~150 nm. In addition, the aerosol absorbs longwave radiation in the lower stratosphere that is roughly proportional to its mass loading. This heating and the availability of reactive surface area leads to changes in stratospheric chemistry [*Heckendorn et al.*, 2009]. Reducing the geoengineered sulfur mass loading by controlling particle size may reduce lower stratospheric heating and thus some of the unintended adverse impacts in the stratosphere.

[4] Volcanoes inject sulfur into the stratosphere almost exclusively as sulfur dioxide (SO_2), which does not itself condense to aerosols. SO_2 is subsequently oxidized to sulfur trioxide (SO_3) within a few weeks [*Rasch et al.*, 2008a]. SO_3 in turn is almost instantaneously (milliseconds) converted to sulfuric acid (H_2SO_4), see auxiliary material Text S1.[1] H_2SO_4 vapor quickly (hours) condenses onto existing aerosols or forms new aerosols by homogeneous nucleation. Most of the recent analyses have assumed that aerosols in stratospheric-aerosol geoengineering would be produced by an analogous process, i.e. the injection of either SO_2 or H_2S gas that is slowly converted to sulfate aerosol. A recent analysis [*Heckendorn et al.*, 2009] suggests that this method may be ineffective because it produces aerosols that are substantially larger than optimal. The added mass accumulates preferentially on larger pre-existing particles either by direct condensation or by homogeneous nucleation followed by coagulation. The net effect is that radiative forcing increases sub-linearly with sulfur emissions, so a large (relative to previous studies) injection rate of 10 Mt-S/yr at the equator and 20 km produces a radiative forcing of only 1.7 W m^{-2}, less than half of what is needed to offset the radiative forcing of a CO_2 doubling [*Heckendorn et al.*, 2009].

2. Aerosol Formation From H_2SO_4 in an Aircraft Plume

[5] We explore the possibility of forming sulfate aerosols in an aircraft plume by emission of H_2SO_4 vapor rather than

[1]Department of Physics and Atmospheric Science, Dalhousie University, Halifax, Nova Scotia, Canada.
[2]Atmospheric and Environmental Research, Inc., Lexington, Massachusetts, USA.
[3]Institute for Atmospheric and Climate Science, ETH Zurich, Zurich, Switzerland.
[4]Energy and Environmental Systems Group, University of Calgary, Calgary, Alberta, Canada.

0094-8276/10/2010GL043975

[1]Auxiliary materials are available in the HTML. doi:10.1029/2010GL043975.

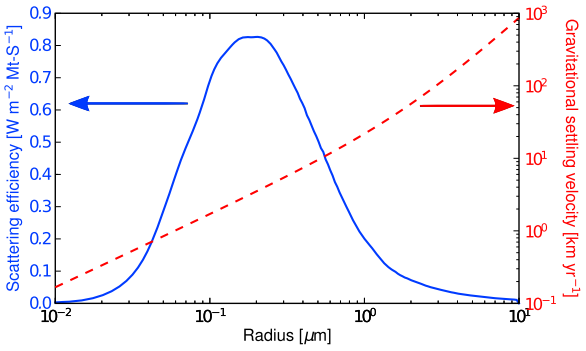

Figure 1. Size dependence of factors that determine the radiative forcing of stratospheric sulphate aerosol. The blue curve and left axis show the solar-band cooling per mass (burden) of sulphate in the stratosphere as a function of aerosol size. The calculation was done assuming monodisperse aerosol and averaging over the solar spectrum. The red curve and right axis show the gravitational settling velocity at a height of 25 km.

SO_2 (Figure S1). (Depending on the injection method, SO_3 vapor may be emitted rather than H_2SO_4, but it is quickly converted to H_2SO_4, see auxiliary material Text S1). Aerosol mass is formed in an aircraft plume when a vapor emitted by the aircraft cools below its condensation point as it mixes with ambient air (similar to the mechanism forming aircraft contrails). More generally, one might exploit the same physics to form a variety of aerosols in the stratosphere by emission of a high-temperature gas-phase substance that has low volatility at ambient temperatures.

[6] To investigate the method, we modeled the formation of sulfate aerosol by the injection of sulfuric acid (H_2SO_4) vapor using an aerosol microphysics model (subsequently called plume model) that follows an expanding parcel in the plume from the time of emission (see auxiliary material Text S1). We integrate the model until the loss of particles by coagulation with ambient particles dominates the self-coagulation, whereupon the AER global 2-D sulfate aerosol model (called AER model and discussed in the next section) becomes the appropriate tool. This hand-off between the models occurs ~2 days after injection (for ambient geoengineered aerosol concentrations of 50 cm^{-3}, Figure S3). Although the hand-off time depends on the concentration of particles in the ambient atmosphere, the model results have only a small sensitivity to the exact details of the hand-off time.

[7] Figure 2 shows the sensitivity of the sulfate aerosol size distribution after 2 days in the plume to the rates of H_2SO_4 emission, plume dilution, aerosol nucleation and condensation (see auxiliary material Text S1). The resulting aerosol size distributions are almost entirely controlled by the emission and plume dilution rates (various colored lines in Figure 2). Size distributions are remarkably insensitive to variation in nucleation and condensation rate coefficients (various line types in Figure 2) because all H_2SO_4 vapor has nucleated or condensed within seconds of emission, so that self-coagulation of new particles smoothes any initial differences in the size distribution. These results are consistent with *Turco and Yu* [1999]. Because the results are quite sensitive to the plume dilution rate, uncertainties in the dilution rates tested here will lead to uncertainties in the resultant size distributions. These results demonstrate that

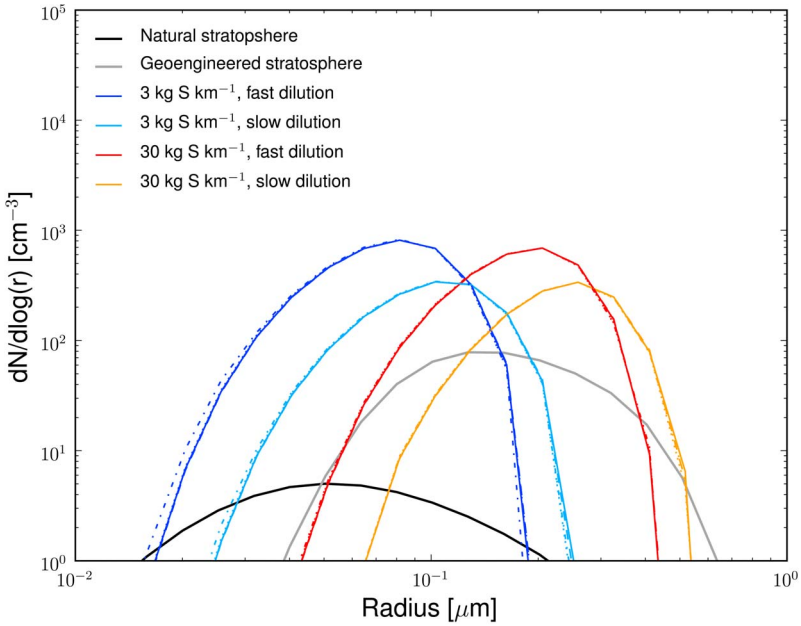

Figure 2. Size distributions of sulfate particles formed in the aircraft plume 2 days after emission of H_2SO_4 derived from the plume model (colored curves) and ambient steady-state size distributions derived from the AER 2D aerosol model at 23 km above the equator without geoengineering (black curve) and with 5 Mt-S yr^{-1} geoengineering (gray curve, from the 95 nm particle case, described later). For each color, there are four cases plotted for scale factors for nucleation of 1 and 10^{-6} and for condensation of 1 and 0.01 (plotted by different line styles, generally overlapping). Ambient particle concentrations with geoengineering of 50 cm^{-3} are used in the plume simulations.

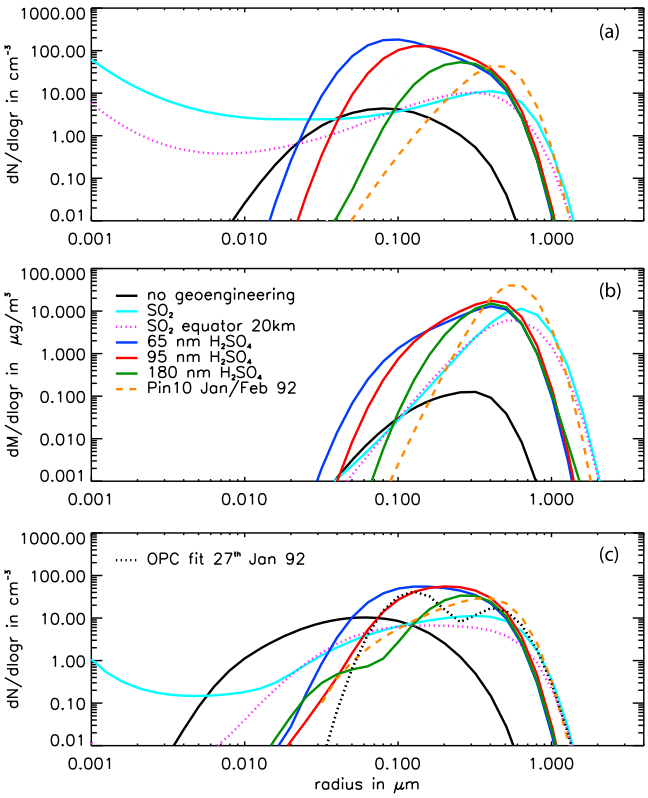

Figure 3. Steady-state annual average aerosol (a) number and (b) mass size distributions at the equator and 23 km and (c) number distributions at 40°N and 17 km predicted by the AER model. Solid black lines: simulations without geoengineering (volcanically quiescent background). Solid colored lines: geoengineering cases with 5 MT S yr^{-1} emission with emissions spread between 30°S and 30°N and 20 and 25 km. Dashed magenta lines: geoengineering case with 5 MT S yr^{-1} emission as SO_2 at a single grid point centered at the equator and 20 km [from *Heckendorn et al.*, 2009]. Dashed orange lines: AER model simulation for January–February 1992 following the Mt. Pinatubo eruption. Dashed black line: size distribution fit to measurements by the optical particle counter (OPC) instrument at 41°N in January 1992.

particles of a desired size could be made by controlling the emission rate and possibly the plume dilution rate (if initial dispersion could be controlled through aircraft and injector design).

3. Stratospheric Aerosol and Radiative Forcing

[8] To model the evolution of aerosol in the stratosphere after the condensation plume has formed and relaxed, we use the AER 2-D aerosol model in the same configuration as was used by *Heckendorn et al.* [2009] to model SO_2 injection. Simulations are run for 10 years, at which point steady-state aerosol concentrations have been reached in the stratosphere. We simulate the injection of 2, 5 and 10 megatons of sulfur per year evenly distributed between 30°N and 30°S and 20 and 25 km altitude continuously in time. The size distributions of injected aerosol are obtained from the plume model with 3 kg S km^{-1} fast and slow dilution cases and the 30 kg S km^{-1} fast dilution case, resulting in number-median radius of 65, 95 or 180 nm with a lognormal width of 1.5, respectively. We compare with cases in which the same amount of sulfur mass is injected in the same region as SO_2.

[9] Figure 3 shows the predicted steady-state aerosol number and mass size distributions (at the equator and 23 km, and 40°N and 17 km) for 5 Mt-S yr^{-1} cases. The SO_2-emission cases in Figure 3a show the presence of a nucleation mode that is missing from the H_2SO_4-emission cases. The SO_2-emission cases also have more large ($r > 1$ μm) particles due to condensation of H_2SO_4 onto accumulation-mode particles and coagulation of nucleated particles with the accumulation-mode particles. The peak mass of the particles (Figure 3b) generated by H_2SO_4 injection is at smaller sizes than particles from SO_2 injection. Comparison of these size distributions with Figure 1 shows that the H_2SO_4-generated particles will have longer stratospheric lifetimes and be more effective scatters than the SO_2-generated particles. Figure 3 also shows aerosol size distributions for January–February 1992 following the eruption of Mt. Pinatubo in the Philippines in June 1991. The AER model calculation from *Heckendorn et al.* [2009] is shown at both the equator and 40°N; additionally, size distributions derived from optical particle counter data [*Deshler et al.*, 1993] are shown at 40°N. For the time and grid points shown, the geoengineering calculations with H_2SO_4 emissions yield aerosol particles of smaller size than the volcanic case, while the SO_2-emission cases lead to particles comparable to or larger than the volcanic case.

[10] Figure 4 shows the steady-state stratospheric sulfur burdens and top of atmosphere solar-band flux changes for various injection scenarios. Our SO_2 reference scenario is more efficient than the *Heckendorn et al.* [2009] scenario ("SO_2 equator, 20 km", replotted here for comparison) because we assume more spatially dispersed SO_2 emissions (30°S–30°N and 20–25 km). Also included for comparison are the stratospheric sulfur burdens computed by *Rasch et al.* [2008b] and the solar flux changes computed by *Robock et al.* [2008], representative of previous modeling that did not include online aerosol microphysics. The sulfur burdens are always higher for the H_2SO_4-injection schemes compared to the SO_2-injection schemes with the same sulfur emission (Figure 4a) due to slower average fall speeds; however, they are still lower than values assumed in previous benchmark studies of geoengineering [*Rasch et al.*, 2008b]. The sulfur burdens from 10 MT yr^{-1} of H_2SO_4 injection are comparable to the maximum sulfur burden obtained following the Pinatubo eruption, which emitted approximately 10 MT-S (not shown). The SO_2-injection cases are extended to 20 Mt-S yr^{-1} due to their lower radiative efficiency.

[11] We use a simple top-of-atmosphere solar-band radiative flux calculation (see auxiliary material Text S1) to determine the relative change in the aerosol radiative forcing between the SO_2- and H_2SO_4-injection schemes (Figure 4b) ignoring feedbacks in atmospheric temperature, chemistry, and dynamics (these effects are of secondary importance, see auxiliary material Text S1). The H_2SO_4-injection cases reach a cooling of −4 W m^{-2} (approximately canceling the global-mean warming from a doubling of CO_2) for less than 10 Mt-S yr^{-1} (approaching previous estimates assumed in the literature [*Robock et al.*, 2008]). On the other-hand, the similar SO_2-injection scheme did not reach −4 W m^{-2} until 19 Mt-S yr^{-1}, and the SO_2-injection scheme at the equator

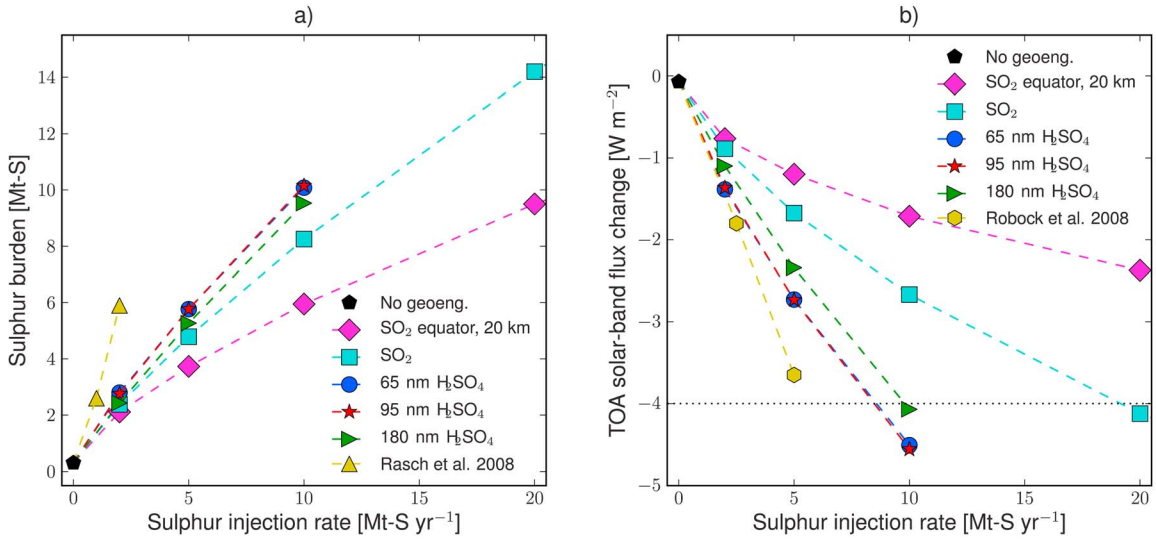

Figure 4. Steady-state (a) stratospheric sulfur burden and (b) top-of-atmospheric solar-band (shortwave) radiative flux change from the stratospheric aerosols as a function of sulfur injection rate. All simulations have emissions evenly distributed between 30°S–30°N and 20–25 km, except results for SO_2 emitted only above the equator (5°S–5°N) at 20 km (19.5–20.5 km). Also included for comparison are the stratospheric sulfur burdens computed by *Rasch et al.* [2008a] (with fixed effective radius of 0.43 μm) and the solar flux changes by *Robock et al.* [2008], both without aerosol microphysics. Black horizontal dotted line in Figure 4b represents the approximate cooling necessary to offset a doubling of CO_2 in the global-mean energy budget.

and 20 km only did not reach this cooling even at 50 Mt-S yr^{-1} showing the great importance of injection location.

4. Discussion and Conclusions

[12] Our results suggest that emission of H_2SO_4 from aircraft may be used to maintain sulfate aerosol burdens and radiative forcings far more efficiently than can be achieved by continuous SO_2 injection. A 50–60% lower sulfur injection rate was required to cool −4 W m^{-2} for H_2SO_4-injection versus SO_2. (This is a 35% reduction in the total mass brought to the stratosphere if H_2SO_4 is carried rather than SO_2, see injection methods in auxiliary material Text S1.) At −4 W m^{-2}, the stratospheric sulfate mass burden for the H_2SO_4-injection cases is about 40% lower than the SO_2 cases. This will lead to less long-wave warming of the lower stratosphere(proportional to the aerosol mass loading) and thus smaller changes in stratospheric chemistry associated with this warming [*Heckendorn et al.*, 2009]. However, all injection methods yield roughly similar aerosol surface area densities for similar radiative coolings, thus reductions in ozone due to surface-area-catalyzed reactions [*Tilmes et al.*, 2008] do not greatly depend on the injection method explored here and could be substantial in all these cases.

[13] Emission of directly condensable vapors, as proposed here, might also be used to produce non-sulfur aerosols with a variety of compositions without natural analogues [*Swihart*, 2003]. An advantage of sulfur is that it mimics a well known natural process, but other compounds might give the same radiative forcing with less mass loading and possibly less impact on stratospheric chemistry and dynamics. For example, alumina (Al_2O_3) has about four times as much scattering per unit volume, so it might be possible to use substantially smaller particle fluxes to achieve the same radiative forcing. Moreover, compared to sulfate, alumina has less infrared absorption and thus would heat the lower stratosphere less, which may produce less ozone loss through this pathway [*Pollack et al.*, 1976; *Jackman et al.*, 1998]. However, chemicals that are less common in nature than sulfate potentially contribute additional risks, both known and unknown.

[14] In order to build understanding of the effectiveness and risks of geoengineering, we first must develop methods that might actually achieve significant negative radiative forcing. Geoengineering by stratospheric aerosol enhancement introduces novel environmental risks and can – at best – partially mask the impacts of greenhouse gases on tropospheric temperatures, whereas issues such as ocean acidification remain unaddressed. This work suggests that the direct formation of aerosols from a plume of low volatility vapors might (a) offer better control of particle size distributions and consequently more efficient negative radiative forcing per unit mass of emission, (b) enable radiative forcings up to −4 W m^{-2} that may be difficult to achieve by continuous emission of SO_2, and finally (c) offer the possibility of using alternative particle compositions that might enable geoengineering with smaller mass loadings and or lower environmental risks [*Blackstock et al.*, 2009]. Beyond the risks arising from the fact that no aerosol geoengineering scheme can fully offset the impacts of greenhouse gases (e.g. ocean acidification and effects on hydrologic cycle), other risks include loss of ozone through heterogeneous chemistry and the impacts of the lower stratospheric warming through absorption of terrestrial radiation [*Matthews and Caldeira*, 2007; *Robock et al.*, 2008; *Tilmes et al.*, 2008, 2009; *Trenberth and Dai*, 2007]. Risk assessment needs to balance the negative side effects with the positive effects from the intended cooling, while efforts

towards rapid greenhouse gas emission reductions should not slacken.

[15] **Acknowledgments.** The authors acknowledge Jay Apt, Beiping Luo, Phil Rasch, Alan Robock, Eugene Rozanov, and Richard Turco and for helpful conversations and feedback. Funding for D.K.W. at AER provided by the NASA ACMAP program.

References

Blackstock, J., et al. (2009), Climate engineering responses to climate emergencies, report, Novim, Santa Barbara, Calif. (Available at http://arxiv.org/pdf/0907.5140)

Caldeira, K., and L. Wood (2008), Global and Arctic climate engineering: Numerical model studies, *Philos. Trans. R. Soc. A*, *366*, 4039–4056.

Deshler, T., B. J. Johnson, and W. R. Rozier (1993), Balloonborne measurements of Pinatubo aerosol during 1991 and 1992 at 41°N, vertical profiles, size distribution and volatility, *Geophys. Res. Lett.*, *20*, 1435–1438, doi:10.1029/93GL01337.

Govindasamy, B., and K. Caldeira (2000), Geoengineering Earth's radiation balance to mitigate CO_2-induced climate change, *Geophys. Res. Lett.*, *27*, 2141–2144, doi:10.1029/1999GL006086.

Govindasamy, B., S. Thompson, P. Duffy, K. Caldeira, and C. Delire (2002), Impact of geoengineering schemes on the terrestrial biosphere, *Geophys. Res. Lett.*, *29*(22), 2061, doi:10.1029/2002GL015911.

Govindasamy, B., K. Caldeira, and P. Duffy (2003), Geoengineering Earth's radiation balance to mitigate climate change from a quadrupling of CO_2, *Global Planet. Change*, *37*, 157–168, doi:10.1016/S0921-8181(02)00195-9.

Heckendorn, P., et al. (2009), The impact of geoengineering aerosols on stratospheric temperature and ozone, *Environ. Res. Lett.*, *4*, 045108, doi:10.1088/1748-9326/4/4/045108.

Jackman, C. H., D. B. Considine, and E. L. Fleming (1998), A global modeling study of solid rocket aluminum oxide emission effects on stratospheric ozone, *Geophys. Res. Lett.*, *25*, 907–910, doi:10.1029/98GL00403.

Keith, D., E. Parson, and M. G. Morgan (2010), Research on global sun block needed now, *Nature*, *463*, 426–427, doi:10.1038/463426a.

Matthews, H. D., and K. Caldeira (2007), Transient climate-carbon simulations of planetary engineering, *Proc. Natl. Acad. Sci. U. S. A.*, *104*, 9949–9954, doi:10.1073/pnas.0700419104.

Pollack, J. B., O. B. Toon, A. Summers, W. Van Camp, and B. Baldwin (1976), Estimates of the climatic impact of aerosols produced by space shuttles, SST's, and other high flying aircraft, *J. Appl. Meteorol.*, *15*, 247–258, doi:10.1175/1520-0450(1976)015<0247:EOTCIO>2.0.CO;2.

Rasch, P. J., et al. (2008a), An overview of geoengineering of climate using stratospheric sulfate aerosols, *Philos. Trans. R. Soc. A*, *366*, 4007–4037.

Rasch, P. J., P. J. Crutzen, and D. B. Coleman (2008b), Exploring the geoengineering of climate using stratospheric sulfate aerosols: The role of particle size, *Geophys. Res. Lett.*, *35*, L02809, doi:10.1029/2007GL032179.

Robock, A., L. Oman, and G. L. Stenchikov (2008), Regional climate responses to geoengineering with tropical and Arctic SO_2 injections, *J. Geophys. Res.*, *113*, D16101, doi:10.1029/2008JD010050.

Shepherd, J., et al. (2009), Geoengineering the climate: Science, governance and uncertainty, report, R. Soc., London.

Swihart, M. T. (2003), Vapor phase synthesis of nanoparticles, *Curr. Opin. Colloid Interface Sci.*, *8*(1), 127–133.

Tilmes, S., R. Muller, and R. Salawitch (2008), The sensitivity of polar ozone depletion to proposed geoengineering schemes, *Science*, *320*, 1201–1204, doi:10.1126/science.1153966.

Tilmes, S., R. R. Garcia, D. E. Kinnison, A. Gettelman, and P. J. Rasch (2009), Impact of geo-engineered aerosols on the troposphere and stratosphere, *J. Geophys. Res.*, *114*, D12305, doi:10.1029/2008JD011420.

Trenberth, K. E., and A. Dai (2007), Effects of Mount Pinatubo volcanic eruption on the hydrological cycle as an analog of geoengineering, *Geophys. Res. Lett.*, *34*, L15702, doi:10.1029/2007GL030524.

Turco, R. P., and F. Yu (1999), Particle size distributions in an expanding plume undergoing simultaneous coagulation and condensation, *J. Geophys. Res.*, *104*, 19,227–19,241, doi:10.1029/1999JD900321.

P. Heckendorn and T. Peter, Institute for Atmospheric and Climate Science, ETH Zurich, CH-8092 Zurich, Switzerland.

D. W. Keith, Energy and Environmental Systems Group, University of Calgary, Calgary, AB T2N 1N4, Canada. (keith@ucalgary.ca)

J. R. Pierce, Department of Physics and Atmospheric Science, Dalhousie University, Halifax, NS B3H 2W3, Canada.

D. K. Weisenstein, Atmospheric and Environmental Research, Inc., Lexington, MA 02421, USA.